NASA Technical Paper 1524

Lubricating and Wear Mechanisms for a Hemisphere Sliding on Polyimide-Bonded Graphite Fluoride Film

Robert L. Fusaro

AUGUST 1979

SUMMARY

The tribological properties of a 440C high-temperature-stainless-steel, hemispherically tipped rider (0.476-cm radius) sliding against polyimide-bonded graphite fluoride films that were 10, 18, and 45 micrometers thick were studied. The films were applied to 440C HT stainless-steel disks that had been roughened by sandblasting to 1.2±0.2 micrometers centerline average (CLA) and were then evaluated in a controlled moist-air atmosphere (10 000 ppm H_2O) at 25° C. Optical microscopy and surface profilometry were used to study the lubricating films, the transfer films, and the wear processes. Observations were made at preset intervals throughout the wear lives of the films by stopping the tests and removing the specimens from the apparatus.

Two lubrication regimes operated for the same load. In the first, the film supported the load and the lubricating mechanism consisted of the shear (plastic flow) of a thin layer of the polyimide-bonded graphite fluoride between the metallic rider and the film surface. In the second, the film did not support the load (it was worn away) and the lubricating mechanism consisted of the shear of very thin films (0.8 μm or less) between flat areas generated on the rider and on sandblasted metallic asperities in the film wear track. The second lubrication regime prevailed throughout most of the film's wear life.

In the second lubrication regime, lubricant was supplied to the metallic flats from two sources: (1) from the valleys between the metallic sandblasted asperities and (2) from the sides of the film wear track. Thus, with thicker films, wear life increased since a greater lubricant supply was available from the sides of the wear track. No detectable wear occurred to the rider in the first lubrication regime. But, after transition to the second regime, rider wear increased with sliding distance at a relatively constant rate. Failure was characterized by the depletion of the polyimide-bonded graphite fluoride from the contact area and by the production of very fine, powdery metallic debris. No galling wear of the surfaces was observed.

INTRODUCTION

The friction, film wear life, and rider wear for 440C high-temperature-stainless-steel riders sliding on polyimide-bonded graphite fluoride films have been studied in a pin-on-disk testing apparatus (refs. 1 and 2). Long wear lives (~3000 kilocycles of

sliding) and low friction coefficients (0.12 to 0.20) were obtained at 25° C in a moist-air atmosphere (50 percent relative humidity). Rider wear rates were also very low (3.4×10^{-17} to 4.7×10^{-17} m^3/m) (ref. 3). In a Falex testing apparatus, similarly formulated films failed after 15.8 minutes (4.6 kilocycles of sliding) (ref. 4). The authors of reference 4 have attributed this short wear life to the films' apparently poor load-carrying capacity. Loads up to 227 kilograms (500 lb) were used in those experiments.

Although there are many applications for solid lubricants where heavy loads are used, there are also many applications for lighter loads. One example is in foil bearings, where loads of 260 kilopascals (37 psi) are typical (ref. 5). Thermal exposure experiments on polyimide-bonded graphite fluoride films (ref. 3) disclosed that this lubricant has a higher thermal stability than the PTFE solid lubricant presently being used in foil bearings. For a number of reasons, including efficiency, there is an advantage in operating these bearings at temperatures higher than those at which they are presently being used, and polyimide-bonded graphite fluoride has potential for this application.

It is puzzling why much longer wear lives were obtained with the pin-on-disk tester than with the Falex tester. Is this due simply to load capacity or do other factors enter into it? In general, the mechanisms by which bonded solid-lubricant films lubricate, wear, and fail are not well understood. Therefore this investigation was conducted to obtain a more fundamental understanding of the mechanisms by which polyimide-bonded graphite fluoride films lubricate and wear and of the phenomena controlling the wear life.

The scope of the investigation included studying the effect of film thickness on wear life, friction coefficient, rider wear rate, and film wear from tests conducted on polyimide-bonded graphite fluoride films applied to sandblasted 440C HT stainless-steel disks. The procedure used was to stop the tests at preset sliding intervals and then to examine what had occurred on the sliding surfaces by optical microscopy at magnifications to 1100. Three film thicknesses were studied: 10, 18, and 45 micrometers. The experimental conditions for the pin-on-disk apparatus were a controlled atmosphere of 50-percent-relative-humidity moist air (10 000 ppm H_2O), a load of 1 kilogram, a sliding speed of 2.6 meters per second (1000 rpm), and a temperature of 25° C.

MATERIALS

Pyralin polyimide (PI-4701) was used in this study. The polyimide was obtained as a thick precursor solution. To provide a sprayable mixture, a thinner consisting of N-methyl-pyrrolidone and xylene was added to it. The polyimide-bonded graphite

fluoride films were prepared by mixing equal parts by weight of polyimide solids (the precursor solution contained 43 percent solids) with graphite fluoride powder. The graphite fluoride used had a fluorine-to-carbon ratio of 1.1. The films were applied to AISI 440C HT stainless-steel disks (1.2 cm thick by 6.3 cm in diam) that had a hardness of Rockwell C-58. The riders used in the friction and wear tests were also made from the 440C HT stainless steel with a hardness of Rockwell C-58.

FRICTION APPARATUS

A hemisphere-on-flat sliding friction and wear apparatus was used to study the lubrication characteristics of the solid-lubricant films. The device is shown in figure 1. The riders were hemispherically tipped pins with a radius of 0.476 centimeter. They were loaded with a 1-kilogram deadweight against a flat, 6.3-centimeter-diameter disk, which was rotated at 1000 rpm. The rider slid on the disk at a radius of 2.5 centimeters at a linear sliding speed of 2.6 meters per second. The friction specimens were enclosed in a chamber so that the atmosphere could be controlled. To obtain the controlled air atmosphere of 10 000 ppm H_2O (~50 percent relative humidity), dry air was mixed with dry air bubbled through water.

PROCEDURE

Surface Preparation and Cleaning

The disk surfaces were roughened by sandblasting to a centerline-average (CLA) roughness of 0.9 to 1.2 micrometers. After surface roughening, the disks were scrubbed with a brush under running tap water to remove the abrasive particles. A water paste of levigated alumina was next rubbed over the surface with a polishing cloth. This was followed by a second scrubbing under running tap water. The disks were rinsed in distilled water; and then clean, dry compressed air was used to quickly dry the surfaces. The disks were stored in a desiccator until they were ready for coating with the solid lubricant.

The riders were washed with ethyl alcohol and then scrubbed with a water paste of levigated alumina. The riders were next rinsed in distilled water and dried with compressed air. Lubricant was not applied to the riders.

Film Application

An artists airbrush was used to apply the polyimide-bonded graphite fluoride films to the disks. The films did not dry rapidly; so only a thin layer was applied at one time to prevent "running." Each thin layer was cured completely before the next layer was applied. The cure was to heat the films at 100° C for 1 hour and then at 300° C for 2 hours.

Three film thicknesses were evaluated in this study: 10, 18, and 45 micrometers. Since each layer applied was from 8 to 13 micrometers thick, it took up to four applications to achieve the desired thicknesses.

Friction and Wear Tests

The procedure for conducting the friction and wear tests was as follows: A rider and disk (coated with the solid-lubricant film) were inserted into the friction apparatus and the test chamber was sealed. The test atmosphere, moist air (10 000 ppm H_2O), was purged through the chamber for 15 minutes before each test. The flow rate was 1500 cubic centimeters per minute, and the chamber volume was 2000 cubic centimeters. After the chamber had been purged for 15 minutes, the disk was set into rotation at 1000 rpm and a 1-kilogram load was gradually applied. The test temperature was 25° C.

Each test was stopped after 1/4 kilocycle (1/4 min) of sliding. After the rider and disk were removed from the friction apparatus, the contact areas were examined by optical microscopy and photographed. Surface profiles of the disk wear tracks were also taken. The rider and disk were then placed back into the apparatus and the test procedure was repeated. The rider was not removed from the holder, and locating-pins in the apparatus ensured that it was returned to its original position. The same was true for the disk.

Each test was stopped and this procedure repeated after sliding intervals of 1/4, 1, 5, 15, 60, 120, 250, 500, 900, 1800, 2800, 3800, and 4400 kilocycles, or when failure occurred. The failure criterion in this study was arbitrarily chosen as a friction coefficient of 0.30. Rider wear was determined by measuring the diameter of the wear scar on the hemispherically tipped rider and then calculating the volume of material worn away.

Analysis of Sliding Surfaces

Optical microscopy was used to study the lubricating films, the transfer films, and the wear particles in this investigation. The surfaces were viewed at magnifications to 1100. At these high magnifications, the depth of focus was very small (~1 μm); this feature was used in measuring the heights of various features on the sliding surfaces, such as film thickness and wear track depth.

The thin films of polyimide-bonded graphite fluoride were transparent. Since illumination and observation of the surfaces were normal to the surfaces, interference fringes could be seen in the films both on the disk wear track and on the rider. Interference fringes showed that solid-lubricant films were present and that the films were smooth and continuous.

RESULTS AND DISCUSSION

Friction and Wear Life

The friction and wear life experiments were conducted at 25^{o} C in a moist-air atmosphere (10 000 ppm H_2O). Figure 2 gives friction traces for 440C HT stainless-steel riders sliding on polyimide-bonded graphite fluoride films of three thicknesses: 10, 18, and 45 micrometers. The friction traces are discontinuous because the tests were stopped at various intervals to make wear measurements and to observe the sliding surfaces with an optical microscope. The experiments were terminated when the friction coefficient reached 0.30, and wear life was defined as the number of sliding revolutions to reach this friction coefficient.

For all three film thicknesses evaluated, the friction coefficient was initially 0.08 to 0.09 and then rose gradually with sliding distance. Eventually the friction coefficient leveled off at a steady-state value of 0.20±0.02. On restart, after the tests had been stopped to measure wear, the friction coefficient was usually lower than it had been at the end of the previous interval. A continuous increase in friction coefficient (from the steady-state value) signified that the films were approaching failure (fig. 2).

Figure 2 shows that thicker films gave longer wear lives. The 10-micrometer-thick film gave a wear life of 980 kilocycles, the 18-micrometer-thick film gave a wear life of 1845 kilocycles, and the 45-micrometer-thick film gave a wear life of 4400 kilocycles. Wear life is shown to be directly proportional to film thickness in figure 3. This result agreed with results of previous experiments conducted on polyimide-bonded molybdenum disulfide films (ref. 6). The wear life of the polyimide-bonded graphite fluoride film was 100 kilocycles per micrometer of film thickness.

Film Wear

Film wear was studied by taking surface profiles of the film wear tracks during the intervals when the tests were stopped. Figure 4 gives surface profiles of these wear tracks on the three films evaluated after 1, 5, and 500 kilocycles of sliding. Profiles are also shown of the wear tracks on each film after failure had occurred. Superimposed on each trace in figure 4 is a surface profile of the 440C HT stainless-steel substrate.

The vertical magnification of the surface profiles is about 50 times the horizontal magnification, giving a distorted view of the surface. The surface profiles show that after 1 kilocycle of sliding very little wear had occurred on the film surfaces. But after only 5 kilocycles of sliding, the films had been worn through and contact with the sandblasted metallic substrate had occurred. Thus, regardless of film thickness, the film had worn through to the metal after 5 kilocycles of sliding. From this point onward, wear was characterized by the gradual increase in wear track width.

Wear of the surfaces was also studied with an optical microscope at magnifications to 1100. In general, the lubricating mechanisms and the appearances of the sliding surfaces were the same regardless of film thickness. Thus to avoid being repetitious, most of the photomicrographs shown are for the 18-micrometer-thick film. Figure 5 gives photomicrographs of the wear track on the 18-micrometer-thick polyimide-bonded graphite fluoride film after sliding intervals of 1/4, 1, 5, and 15 kilocycles. Figure 6 gives higher magnification photomicrographs of the wear tracks for the same sliding intervals.

As the rider contacts the film, the film must either wear or deform elastically or plastically until it supports the load. The surface profiles of figure 4 and the photomicrographs of figures 5(a) and (b) show that initially very little wear occurred. However, figures 5(c) and 6(a) to (c) show that the contact stress and the sliding stress induced cracking and crumbling of the film. At first, the cracks were very small (fig. 6(a)); but, as sliding progressed, they propagated and enlarged and eventually led to crumbling and the complete breakup of the film on the wear tracks (figs. 5(c) and 6(c)).

Once the original film was worn away, asperities on the 440C HT stainless-steel substrate interacted with the rider and helped to support the load (figs. 5(d) and 6(d)). Figures 7 and 8 illustrate that the lubricating mechanism of polyimide-bonded graphite fluoride films (after the original film was worn away) was very similar to the lubricating mechanism for rubbed (burnished) graphite fluoride films (ref. 7).

The lubricating mechanism for rubbed graphite fluoride films consisted of the shear of very thin films of graphite fluoride between flat plateaus on the sandblasted metallic substrate and the metallic rider. The lubricating mechanism was dynamic; the graphite fluoride was supplied to the plateaus from the valleys between them, and

very thin films essentially flowed across the plateaus and were deposited in the following valley.

Figure 7 shows photomicrographs of polyimide-bonded graphite fluoride wear tracks after 60, 500, 900, and 1800 kilocycles of sliding. The figure reveals that two things happened in the wear track as a function of sliding duration. First, the area of each individual plateau increased, indicating the truncation of the metallic asperities; and second, the wear track width increased, indicating rider wear.

Figure 8 shows that the bright areas of figure 7 are flat metallic plateaus covered with extremely thin films of polyimide-bonded graphite fluoride. The polyimide-bonded graphite fluoride can be discerned on the metallic plateaus by color changes and interference fringes.

Rider Transfer and Wear

Photomicrographs of rider contact areas that correspond to the film wear tracks of figure 5 are shown in figure 9. During the sliding interval of 0 to 15 kilocycles, none or very little interaction occurred between the metallic asperities on the disk substrate and the rider. Thus essentially no wear occurred to the rider, and only a thin transfer film of polyimide-bonded graphite fluoride was present on the rider.

Figure 10 shows high-magnification photomicrographs of the transfer after sliding intervals of 1/4, 5, and 15 kilocycles. After 1/4 kilocycle of sliding (fig. 10(a)) the transfer film looked milky colored, suggesting that it was thinner than the wavelength of light (0.4 μm). On continued sliding the transfer film tended to get thicker, and after 15 kilocycles of sliding (fig. 10(c)) broad, multicolored interference bands covered the surface. Because the predominant colors of the bands were red, orange, yellow, and green, the thicknesses were probably from 0.8 to 0.5 micrometer.

Once the polyimide-bonded graphite fluoride film was worn through and the rider made contact with the sandblasted asperities on the disk, wear occurred to the rider. Figure 11 shows the wear scar on the hemispherically tipped rider after 60, 500, 900, and 1800 kilocycles of sliding. These photomicrographs correspond to those of the film wear tracks in figure 7.

During each interval that the tests were stopped, rider wear was determined by measuring the diameter of the wear scar on the hemispherically tipped riders and from that calculating the volume of material removed. Figure 12 gives rider wear as a function of sliding duration for the three film thicknesses. The rate of rider wear was also calculated, and table I gives those data for the three film thicknesses (10, 18, and 45 μm) in terms of wear volume per unit distance of sliding.

In general, the thicker films (18 and 45 μm) gave a lower wear rate than the thinner film (10 μm). This lower wear rate was probably caused by the sides of the film wear track partially supporting the load and thus lessening the load on the metallic asperities (fig. 4).

A transient high wear rate occurred for the 10-micrometer-thick film between 5 and 15 kilocycles of sliding and for the 18-micrometer-thick film between 60 and 120 kilocycles of sliding, when a large number of virgin asperities first contacted the rider and attenuated the wear. With the 18-micrometer-thick film the sides of the film helped to support the load, and the transient high wear was not as severe and occurred later. The 45-micrometer-thick film did not show this transient high wear since the asperities made contact with the rider gradually because of the thickness of the film.

When metallic-asperity contact occurred, the transfer film to the rider was much thinner and less continuous than when sliding was completely on the polyimide-bonded graphite fluoride film. Figure 13 shows high-magnification photomicrographs of transfer films on various regions of the rider scars; they correspond to the low-magnification photomicrographs of figure 11. Figure 13(a) shows the scar exit region after 60 kilocycles of sliding. The polyimide-bonded graphite fluoride flowed across the rider scar and tended to coalesce into a thicker film in the exit. Figure 13(b) shows the scar entrance region after 500 kilocycles of sliding. The polyimide-bonded graphite fluoride built up in the entrance region and was sheared thinner as it entered the contact zone. Interference fringes were evident in the entrance region as the polyimide-bonded graphite fluoride entered the contact zone. Interference fringes suggest that the polyimide-bonded graphite fluoride wear debris had coalesced into a very smooth, continuous film in the entrance before it entered the contact zone.

As sliding continued, the general appearance of the transfer film did not change, except that it may have gotten a little thinner (fig. 13(c)). Failure appeared to be caused by lubricant depletion. Figure 13(d) shows the entrance region (of the 18-μm-thick film) after 1800 kilocycles of sliding. Since this test failed at 1845 kilocycles of sliding, this photomicrograph was taken very near failure. The major difference between the rider scar appearance at this point and previous observations was that the scar entrance region was depleted of polyimide-bonded graphite fluoride. This, along with the valleys in the wear track of the sandblasted disk becoming depleted of polyimide-bonded graphite (fig. 8(d)), suggested that lubricant depletion was the primary cause of failure.

In this investigation, wear life was arbitrarily defined as the number of sliding revolutions it took to reach a friction coefficient of 0.30. Observation of the surfaces by optical microscopy revealed that this was a good choice since, when this friction coefficient was reached, the sliding surfaces looked very different from the very thin flowing films found during good lubrication.

Figure 14 shows photomicrographs of the rider contact area and the film wear track area on the 45-micrometer-thick film after failure occurred. The photomicrographs also typify what happened on the 10- and 18-micrometer-thick films. The depletion of the polyimide-bonded graphite fluoride in various regions on the wear track resulted in the excessive production of extremely fine metallic wear particles. The resulting powdery mixture extended in a band (or bands) that ran around the entire circumference of the disk wear track. A matching band was found on the rider.

Lubricating and Wear Mechanisms

References 8 and 9 determined the wear mechanism of polyimide films without any solid-lubricant additions to be one of gradual wear through the film. At 25° C the wear rate of the polyimide film was 4×10^{-6} square centimeter per kilocycle.

In this study, when the solid lubricant graphite fluoride was added to the polyimide in a 1-to-1 weight ratio, the films would only support a load of 1 kilogram for a short time. Cracking and crumbling of the films resulted and the rider quickly wore through the films. Thus this lubricating mechanism (gradual wear through the film) lasted only a short time. Once the original film was worn through, the rider came into contact with the sandblasted asperities of the metallic substrate and wear occurred to both the rider and the asperity tips. Extremely flat areas were worn on both surfaces, and a very thin secondary film was formed on the substrate. The formation of this secondary film constitutes the second mechanism by which polyimide-bonded graphite fluoride films (and solid-lubricant films, in general) provide lubrication.

Figure 15, an idealized schematic drawing of the sliding surfaces, illustrates the second lubricating mechanism. This lubricating mechanism consisted of very thin films of polyimide-bonded graphite fluoride being sheared between the flat area on the rider and the flat areas (plateaus) on the metallic asperities of the substrate. Thus, the lubricating mechanism was dynamic. The lubricant was supplied to the plateaus from the valleys between the asperities, and thin films of polyimide-bonded graphite fluoride essentially flowed across the plateaus and were deposited in a flowing valley.

A similar phenomenon occurred on the rider. The lubricant was supplied to the contact area from the buildup of worn polyimide-bonded graphite fluoride particles in the entrance region. The polyimide-bonded graphite fluoride was compacted and compressed (by the converging hemisphere-on-flat geometry) as it moved toward the contact zone and eventually coalesced into a very thin film that flowed across the flat rider scar and was eventually deposited in the exit region.

Lubricant was supplied to the sliding surfaces from two sources: from the valleys between the sandblasted metallic asperities on the disk, and from the sides of the film

wear track. In fact, wear life was directly proportional to film thickness, which indicates the importance of the lubricant being fed into the contact zone from the sides of the wear track.

Failure was due to the depletion of lubricant film from the contact zone. Transverse flow out of the contact zone and possible chemical decomposition of the lubricant itself resulted in the valleys becoming depleted of lubricant (fig. 8(d)). As depletion occurred, friction increased and black powdery metallic material covered both sliding surfaces (fig. 13).

As long as the metallic, hemispherically tipped rider slid on the polyimide-bonded graphite fluoride film with no interaction between the rider and the sandblasted asperities, no detectable wear occurred to the rider (fig. 9). Only film transfer was observed. Interaction with the sandblasted asperities caused the rider to wear. The thicker the film, the lower the rider wear rates obtained - most likely because the sides of the wear track helped to support the load and there was less load on the metallic asperities.

SUMMARY OF RESULTS

Friction, wear, surface profilometry, and optical microscopy studies on the effect of sliding a hemispherically tipped rider (0.476-cm radius) against polyimide-bonded graphite fluoride films (10, 18, and 45 μm thick) gave the following results:

1. Two lubrication regimes operated with polyimide-bonded graphite fluoride films.

a. First, when the film supported the load, the lubricating mechanism consisted of the shear (plastic flow) of a thin layer of lubricant between the metallic rider and the film surface.

b. Second, when the film did not support the load (it was worn away), the lubricating mechanism consisted of the shear of thin films of polyimide-bonded graphite fluoride between flat areas generated on the rider and sandblasted metallic asperities in the film wear track. The second regime was predominant in these tests.

2. In the second lubrication regime, lubricant was supplied to the metallic flats from two sources: from the valleys between the metallic sandblasted asperities, and from the sides of the film wear track. Thus as film thickness increased, wear life also increased. In fact, wear life was directly proportional to film thickness at a rate of 100 kilocycles of sliding per micrometer of film thickness.

3. In the first lubrication regime, no detectable rider wear occurred; but after transition to the second lubrication regime, rider wear increased with sliding distance at a relatively constant rate.

4. Failure (high friction and rider wear rates) was characterized by the depletion of the polyimide-bonded graphite fluoride from the contact area and by the production of a very fine powdery metallic debris. No galling wear of the surfaces was observed.

Lewis Research Center,
National Aeronautics and Space Administration,
Cleveland, Ohio, April 25, 1979,
505-04.

REFERENCES

1. Fusaro, Robert L.; and Sliney, Harold E.: Lubricating Characteristics of Polyimide-Bonded Graphite Fluoride and Polyimide Thin Films. ASLE Trans. vol. 16, no. 3, July 1973, pp. 189-196.

2. Fusaro, Robert L.; and Sliney, Harold E.: Graphite Fluoride as a Solid Lubricant in a Polyimide Binder. NASA TN D-6714, 1972.

3. Fusaro, Robert L.: Effect of Thermal Exposure on Lubricating Properties of Polyimide Films and Polyimide-Bonded Graphite Fluoride Films. NASA TP-1125, 1978.

4. McConnell, B. D.; Snyder, C. E.; and Strang, J. R.: Analytical Evaluation of Graphite Fluoride and Its Lubrication Performance Under Heavy Loads. Lubr. Eng., vol. 33, no. 4, Apr. 1977, pp. 184-190.

5. Koepsel, Warren F.: Gas Lubricated Foil Bearing Development for Advanced Turbomachines. AFAPL-TR-76-114. Vol. 1, Air Force Aero Propulsion Lab., 1977. (AD-A042980).

6. Hopkins, Vern; and Campbell, Mahlon: Film Thickness Effect on the Wear Life of a Bonded Solid Lubricant Film. Lubr. Eng., vol. 25, no. 1, Jan. 1, 1969, pp. 15-24.

7. Fusaro, Robert L.: Lubrication and Failure Mechanisms of Graphite Fluoride Films. NASA TP-1197, 1978.

8. Fusaro, Robert L.: Polyimide Film Wear - Effect of Temperature and Atmosphere. NASA TN D-8231, 1976.

9. Fusaro, Robert L.: Effect of Atmosphere and Temperature on Wear, Friction, and Transfer of Polyimide Films. ASLE Trans., vol. 21, no. 2, Apr. 1978, pp. 125-133.

TABLE I. - EFFECT OF FILM THICKNESS ON RIDER WEAR RATE FOR RIDERS SLIDING ON POLYIMIDE-BONDED GRAPHITE FLUORIDE FILMS APPLIED TO SANDBLASTED 440C HT STEEL DISKS

Sliding interval, kilocycles	Film thickness, μm		
	10	18	45
	Rider wear rate, m^3/m		
0 to 1	None	None	None
1 to 5	0.60×10^{-15}	None	None
5 to 15	1.19×10^{-15}	None	None
15 to 60	$.13\times10^{-15}$	0.083×10^{-15}	0.069×10^{-15}
60 to 120	$.12\times10^{-15}$	$.150\times10^{-15}$	$.056\times10^{-15}$
120 to 250	$.14\times10^{-15}$	$.043\times10^{-15}$	$.023\times10^{-15}$
250 to 500	$.51\times10^{-15}$	$.034\times10^{-15}$	$.025\times10^{-15}$
500 to 900	$.75\times10^{-15}$	$.190\times10^{-15}$	$.047\times10^{-15}$
900 to 1800	[a]2.70×10^{-15}	1.000×10^{-15}	$.150\times10^{-15}$
1800 to 2800	----------	[b]2.300×10^{-15}	$.330\times10^{-15}$
2800 to 3800	----------	----------	$.640\times10^{-15}$
3800 to 4400	----------	----------	$.880\times10^{-15}$

[a]Failure occurred at 980 kilocycles.
[b]Failure occurred at 1845 kilocycles.

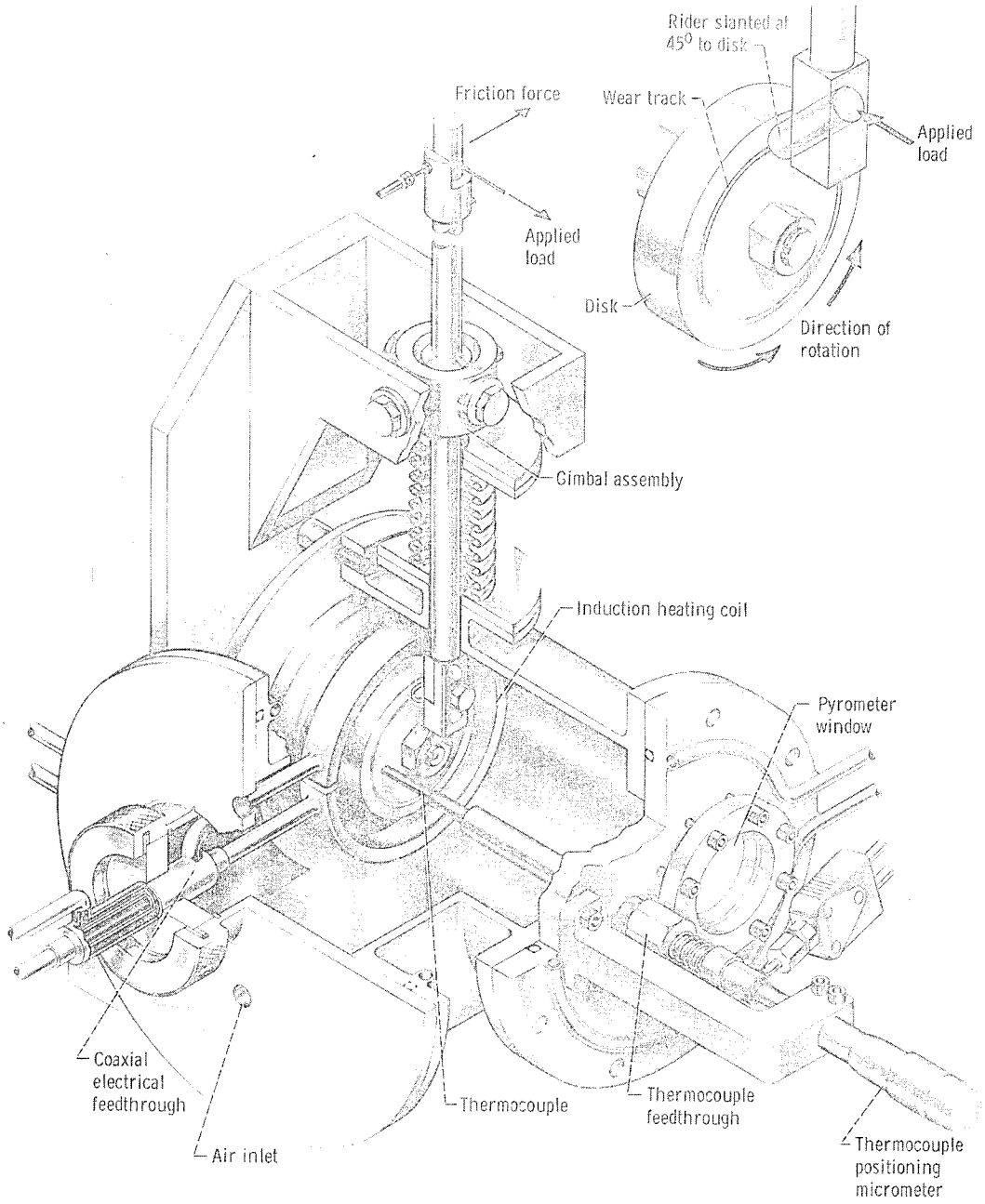

Figure 1. - Friction and wear testing device.

CD-12384-26

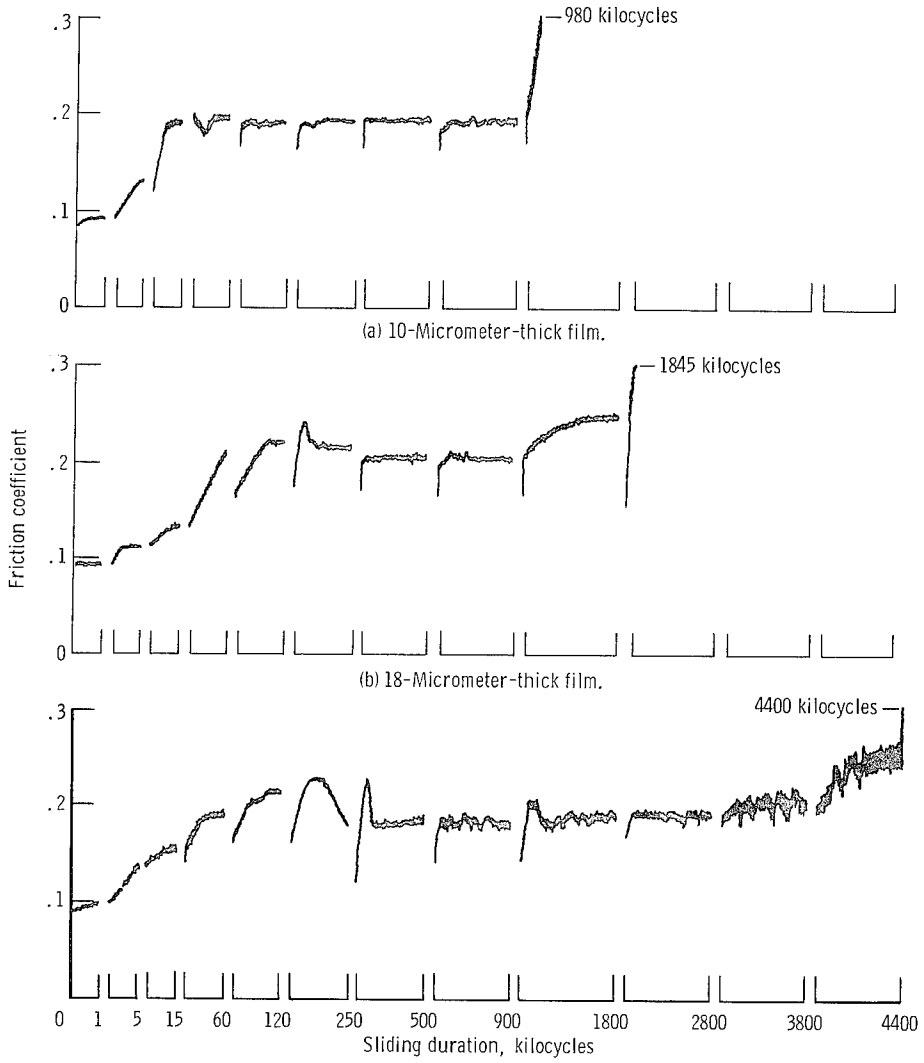

Figure 2. - Friction traces for 440C HT stainless-steel riders sliding on polyimide-bonded graphite fluoride films 10, 18, and 45 micrometers thick. Load, 1 kilogram; sliding speed, 2.6 meters per second (1000 rpm); temperature, 25^0 C; atmosphere, moist air (10 000 ppm H_2O).

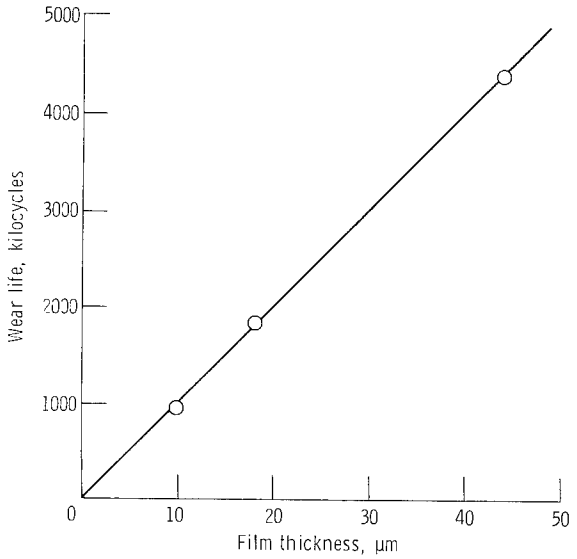

Figure 3. - Wear life as function of polyimide-bonded graphite fluoride film thickness. Rider and disk substrate material, 440C HT stainless steel; rider radius, 0.476 centimeter (hemispherically tipped); load, 1 kilogram; sliding speed, 2.6 meters per second (1000 rpm); temperature, 25° C; atmosphere, moist air (10 000 ppm H_2O).

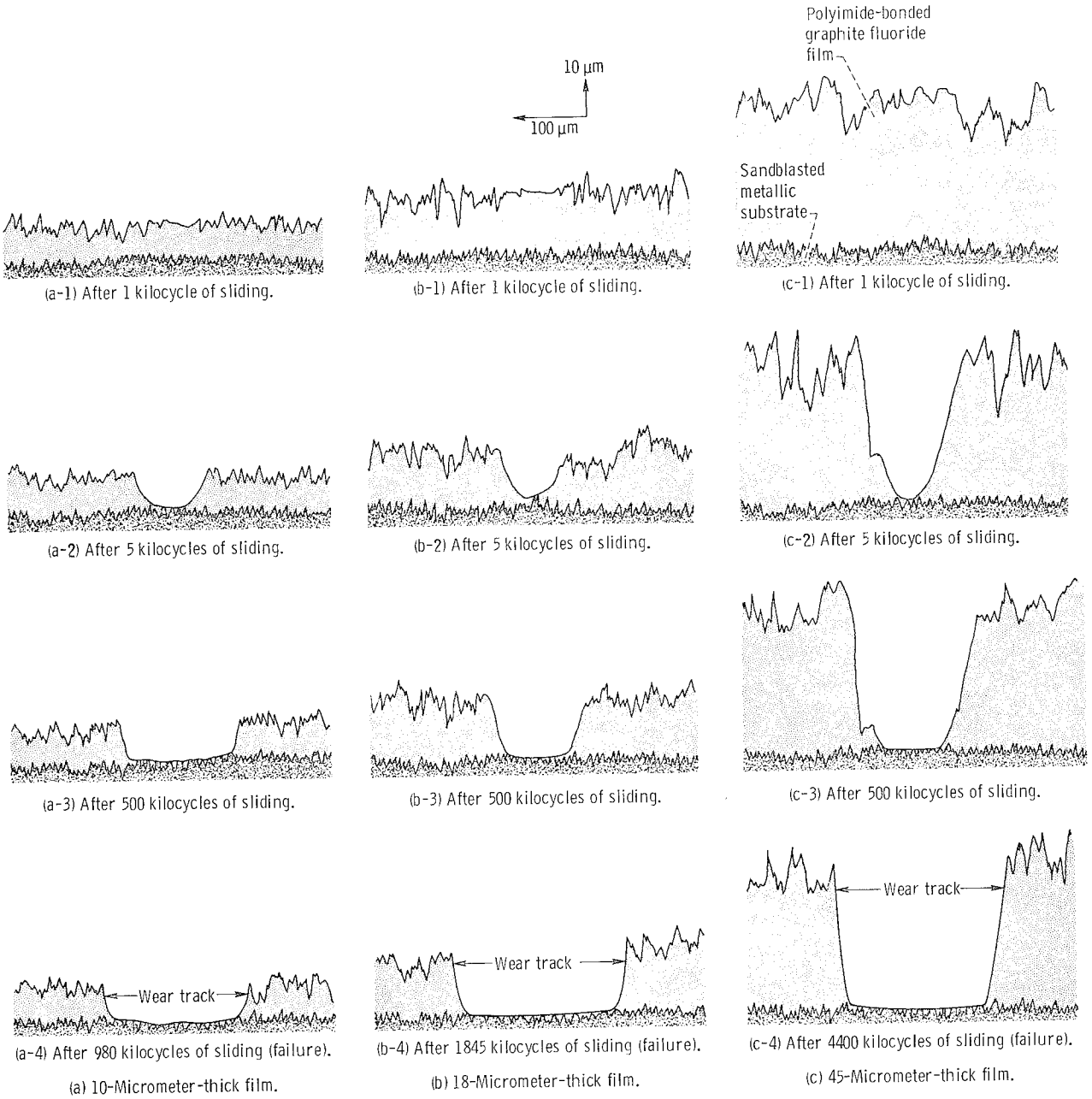

(a-1) After 1 kilocycle of sliding.
(b-1) After 1 kilocycle of sliding.
(c-1) After 1 kilocycle of sliding.
(a-2) After 5 kilocycles of sliding.
(b-2) After 5 kilocycles of sliding.
(c-2) After 5 kilocycles of sliding.
(a-3) After 500 kilocycles of sliding.
(b-3) After 500 kilocycles of sliding.
(c-3) After 500 kilocycles of sliding.
(a-4) After 980 kilocycles of sliding (failure).
(b-4) After 1845 kilocycles of sliding (failure).
(c-4) After 4400 kilocycles of sliding (failure).
(a) 10-Micrometer-thick film.
(b) 18-Micrometer-thick film.
(c) 45-Micrometer-thick film.

Figure 4. - Surface profiles of the wear tracks on polyimide-bonded graphite fluoride films of three thicknesses after various sliding intervals. Rider and disk substrate material, 440C HT stainless steel; rider radius, 0.476 centimeter (hemispherically tipped); load, 1 kilogram; sliding speed, 2.6 meters per second (1000 rpm); temperature, 25° C; atmosphere, moist air (10 000 ppm H_2O).

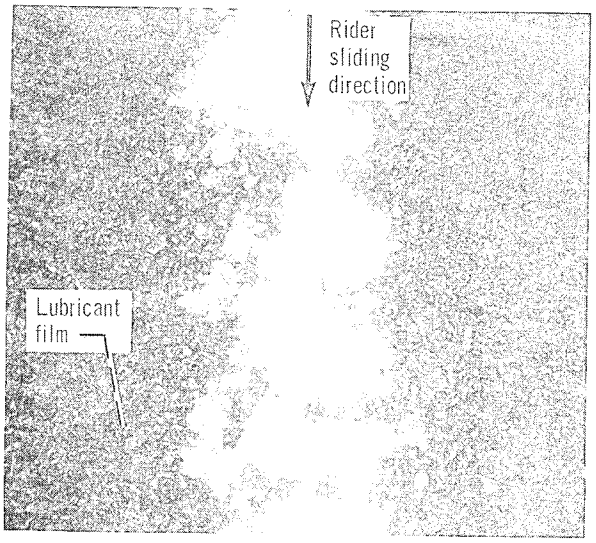

(a) After ¼ kilocycle of sliding.

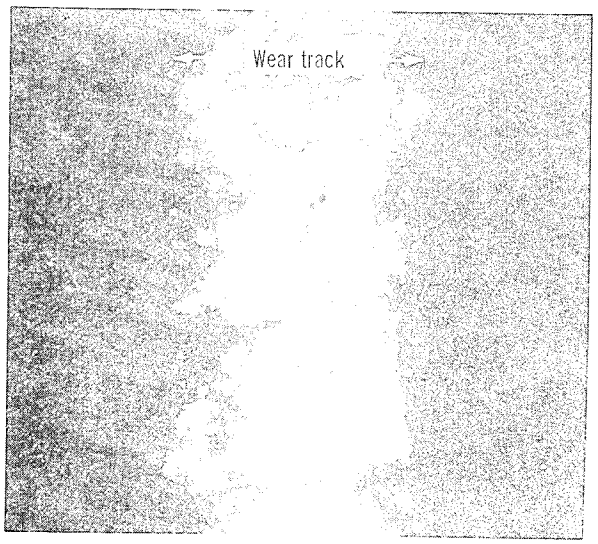

(b) After 1 kilocycle of sliding.

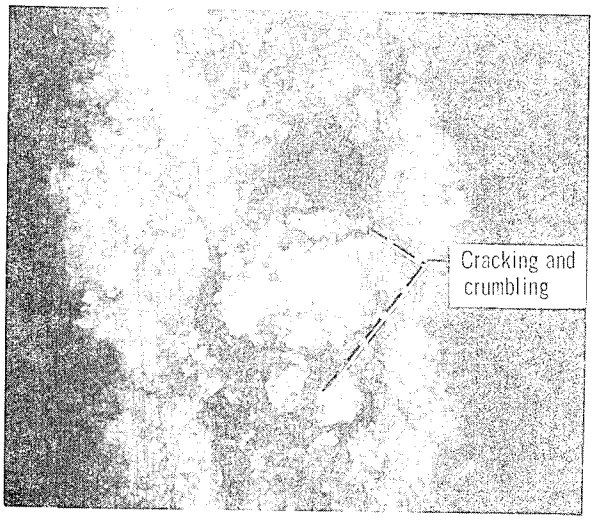

(c) After 5 kilocycles of sliding.

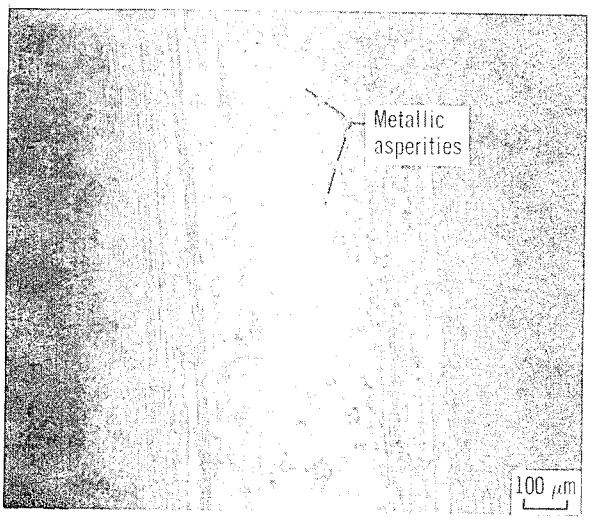

(d) After 15 kilocycles of sliding.

Figure 5. - Photomicrographs of wear track on 18-micrometer-thick polyimide-bonded graphite fluoride film after sliding intervals of ¼, 1, 5, and 15 kilocycles. Rider and substrate material, 440C HT stainless steel; rider radius, 0.476 centimeter (hemispherically tipped); load, 1 kilogram; sliding speed, 2.6 meters per second (1000 rpm); temperature, 25° C; atmosphere, moist air (10 000 ppm H_2O).

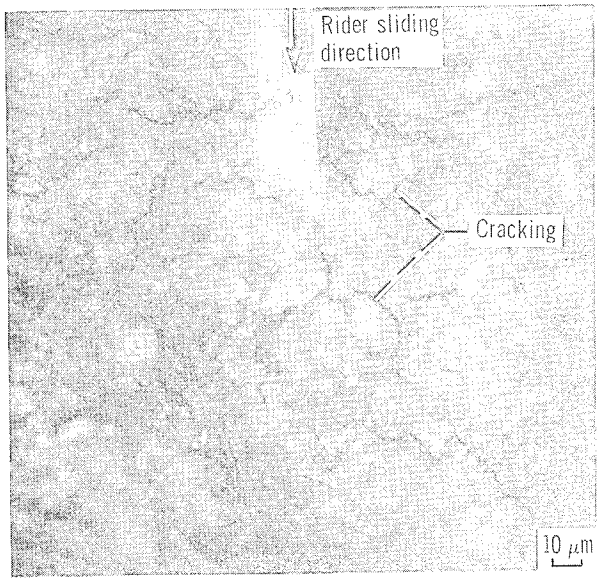

(a) After ¼ kilocycles of sliding.

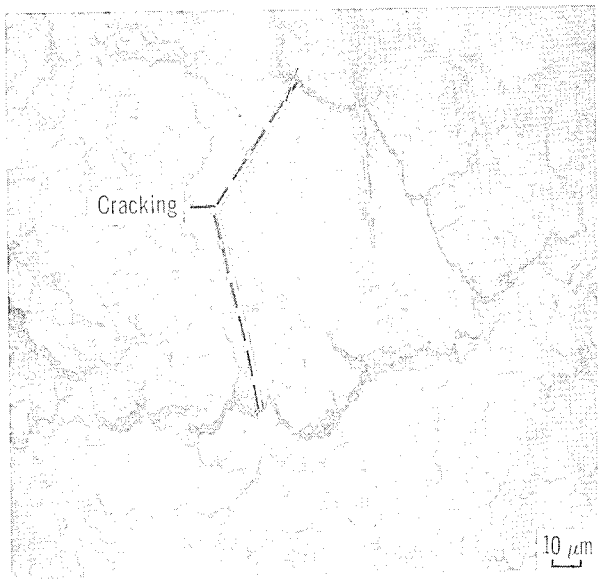

(b) After 1 kilocycle of sliding.

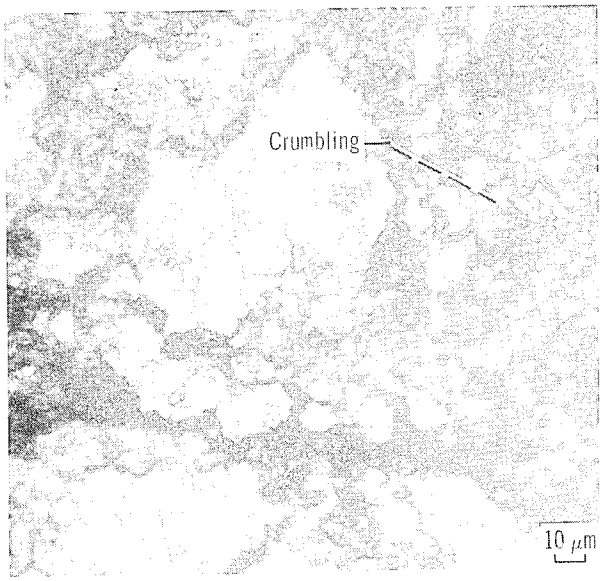

(c) After 5 kilocycles of sliding.

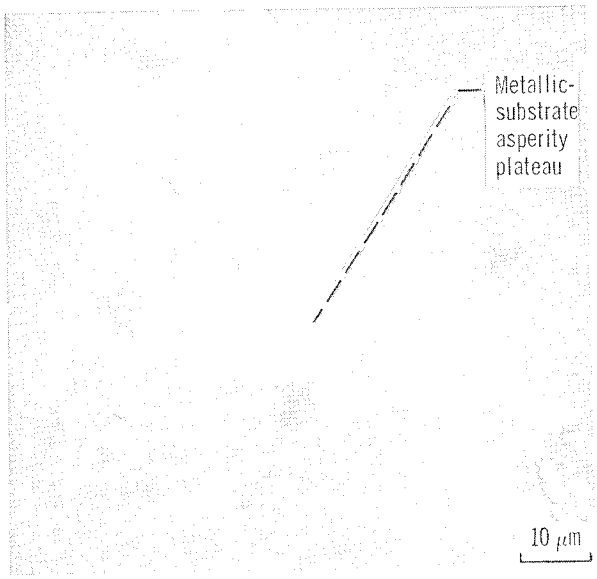

(d) After 15 kilocycles of sliding.

Figure 6. - High-magnification photomicrographs of central area of wear track on 18-micrometer-thick polyimide-bonded graphite fluoride film after sliding intervals of ¼, 1, 5, and 15 kilocycles. Rider and disk substrate material, 440C HT stainless steel; rider radius, 0.476 centimeter (hemispherically tipped); load, 1 kilogram; sliding speed, 2.6 meters per second (1000 rpm); temperature, 25° C; atmosphere, moist air (10 000 ppm H_2O).

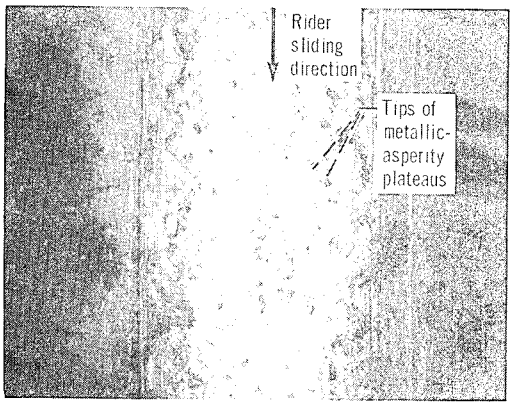

(a) After 60 kilocycles of sliding.

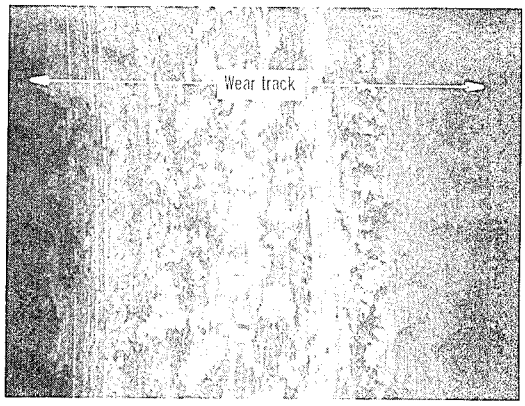

(b) After 500 kilocycles of sliding.

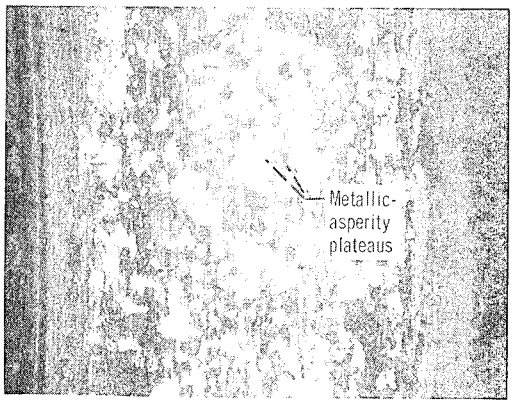

(c) After 900 kilocycles of sliding.

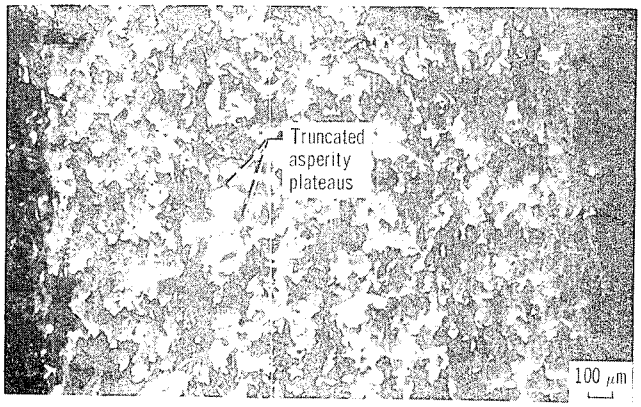

(d) After 1800 kilocycles of sliding.

Figure 7. - Photomicrographs of wear track on 18-micrometer-thick polyimide-bonded graphite fluoride film after sliding intervals of 60, 500, 900, and 1800 kilocycles. Rider and disk substrate material, 440C HT stainless steel; rider radius, 0.476 centimeter (hemispherically tipped); load, 1 kilogram; sliding speed, 2.6 meters per second (1000 rpm); temperature, 25° C; atmosphere, moist air (10 000 ppm H_2O).

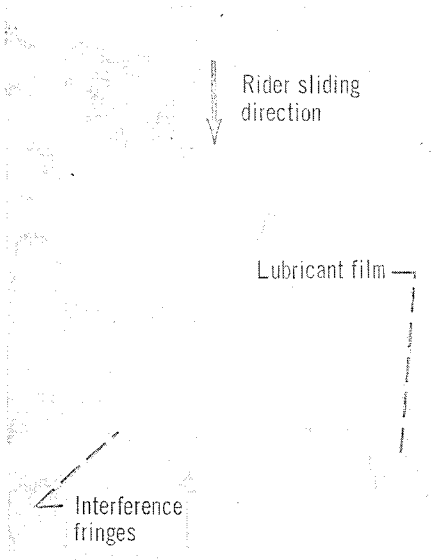

(a) After 60 kilocycles of sliding.

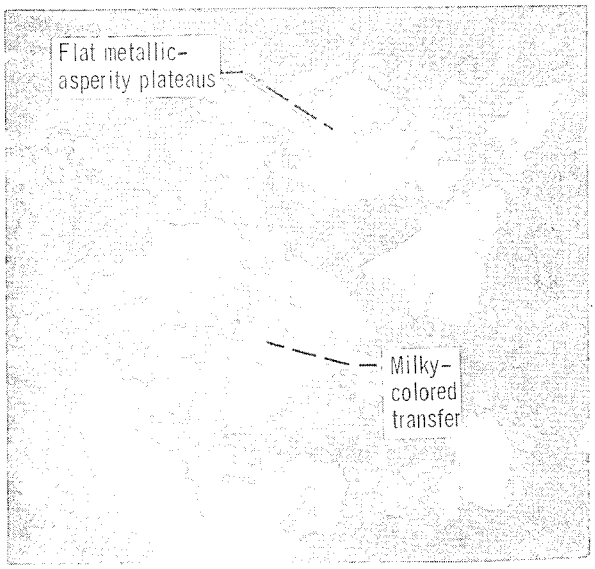

(b) After 500 kilocycles of sliding.

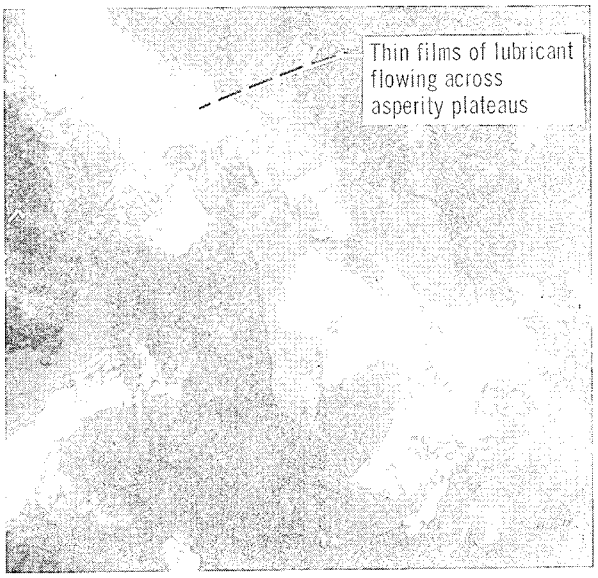

(c) After 900 kilocycles of sliding.

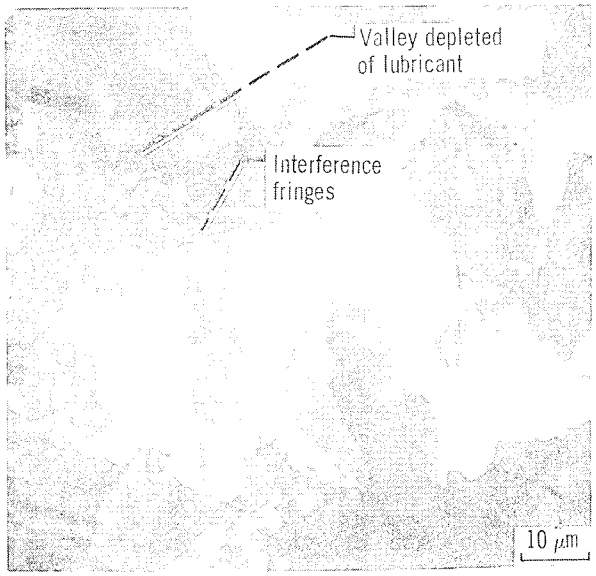

(d) After 1800 kilocycles of sliding.

Figure 8. - High-magnification photomicrographs of central portion of wear track on 18-micrometer-thick polyimide-bonded graphite fluoride film after sliding intervals of 60, 500, 900, and 1800 kilocycles. Rider and disk substrate material, 440C HT stainless steel; rider radius, 0.476 centimeter (hemispherically tipped); load, 1 kilogram; sliding speed, 2.6 meters per second (1000 rpm); temperature, 25° C; atmosphere, moist air (10 000 ppm H_2O).

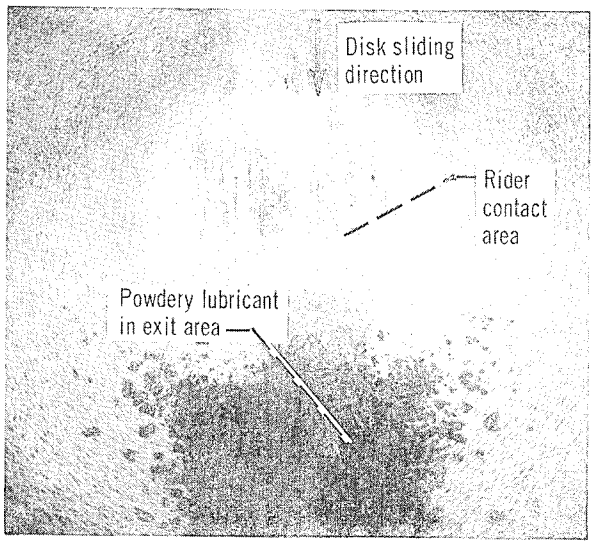

(a) After ¼ kilocycle of sliding.

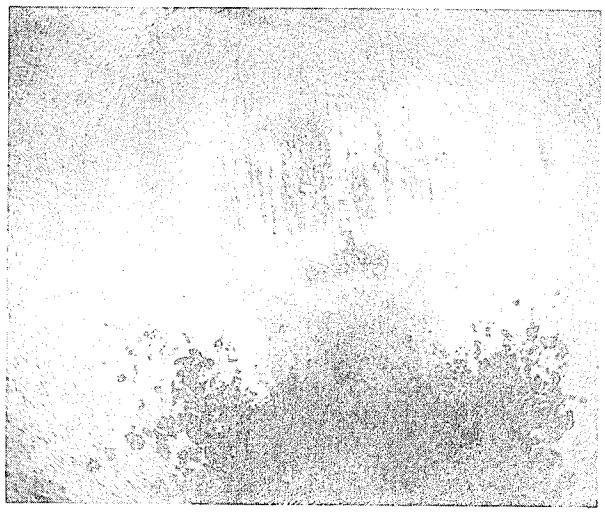

(b) After 1 kilocycle of sliding.

(c) After 5 kilocycles of sliding.

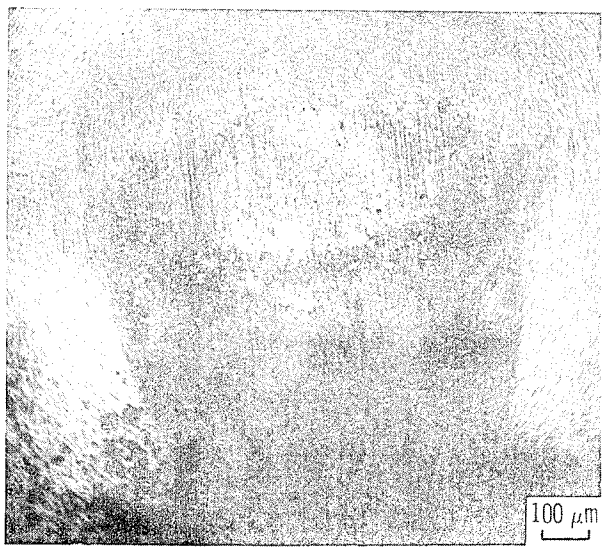

(d) After 15 kilocycles of sliding.

Figure 9. - Photomicrographs of 440C HT stainless-steel-rider contact areas after ¼, 1, 5, and 15 kilocycles of sliding on 18-micrometer-thick polyimide-bonded graphite fluoride film. Substrate material, 440C HT stainless steel; load, 1 kilogram; sliding speed, 2.6 meters per second (1000 rpm); temperature, 25° C; atmosphere, moist air (10 000 ppm H_2O).

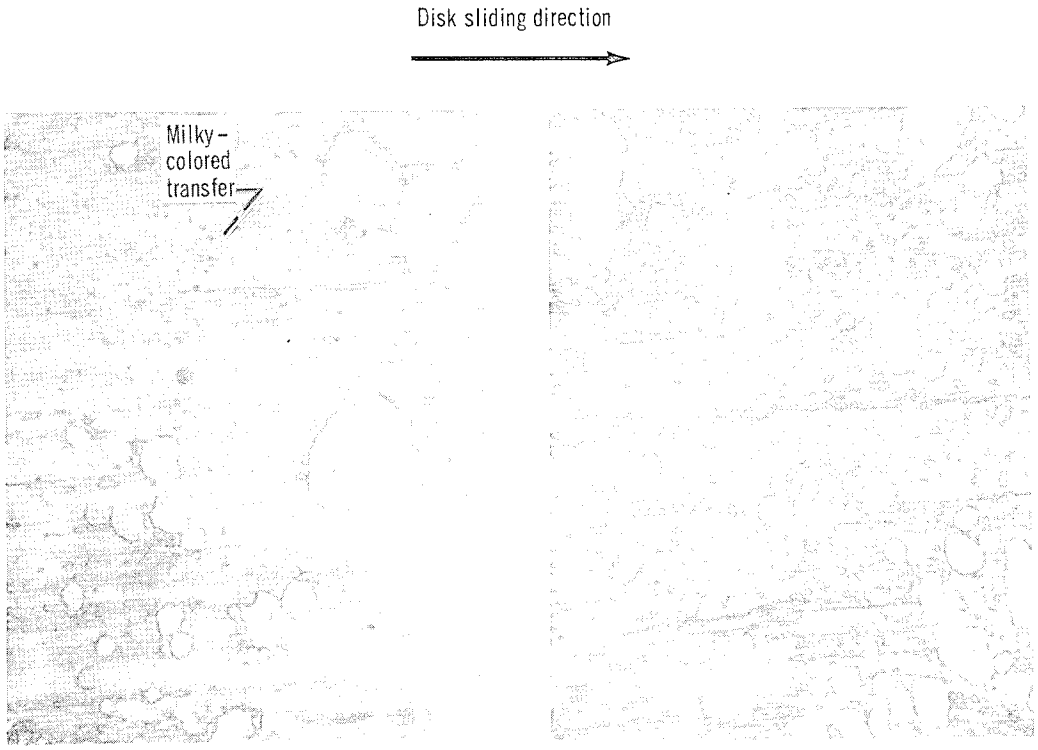

(a) After ¼ kilocycle of sliding.

(b) After 5 kilocycles of sliding.

(c) After 15 kilocycles of sliding.

Figure 10. - High-magnification photomicrographs of typical rider transfer after ¼, 5, and 15 kilocycles of sliding on polyimide-bonded graphite fluoride films. Rider and disk substrate material, 440C HT stainless steel; rider radius, 0.476 centimeter (hemispherically tipped); load, 1 kilogram; sliding speed, 2.6 meters per second (1000 rpm); temperature, 25° C; atmosphere, moist air (10 000 ppm H_2O).

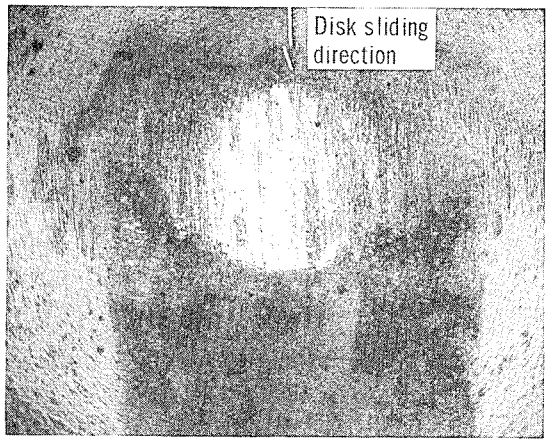

(a) After 60 kilocycles of sliding.

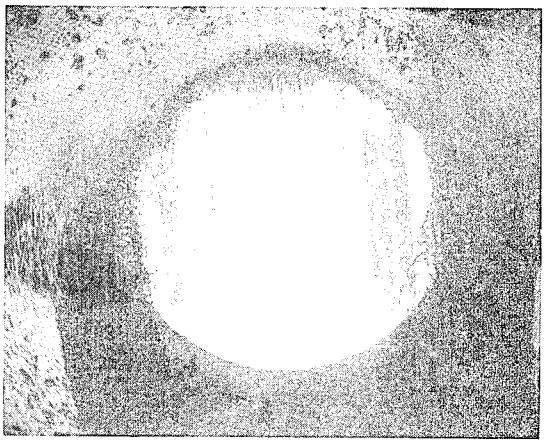

(b) After 500 kilocycles of sliding.

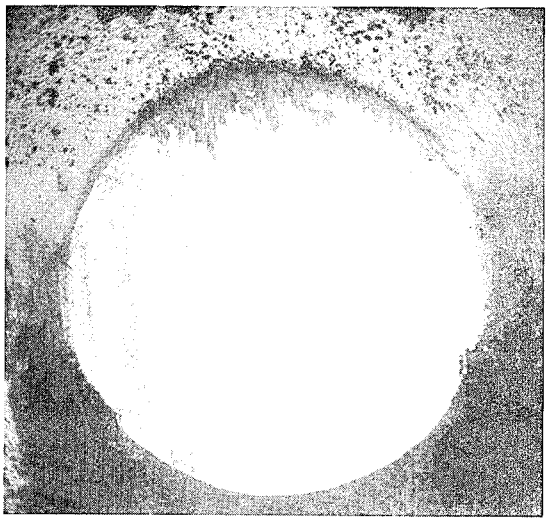

(c) After 900 kilocycles of sliding.

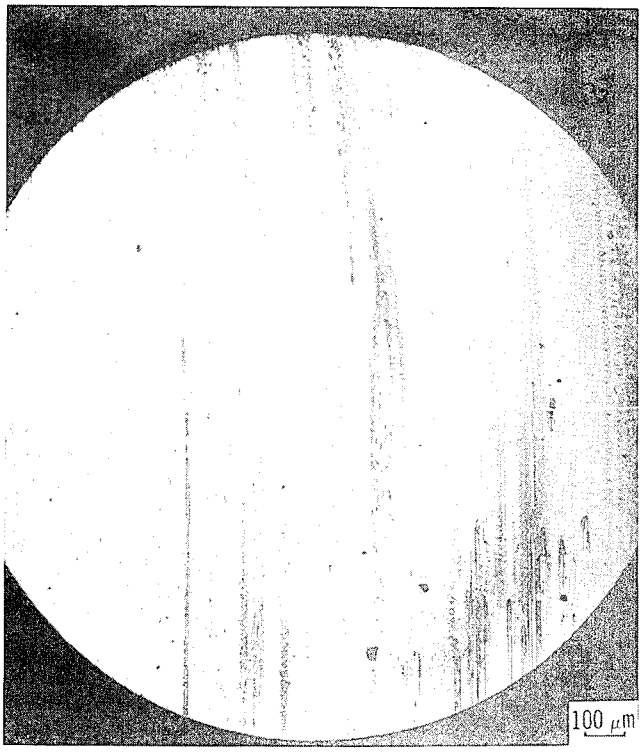

(d) After 1800 kilocycles of sliding.

Figure 11. - Photomicrographs of 440C HT stainless-steel-rider contact areas after 60, 500, 900, and 1800 kilocycles of sliding on 18-micrometer-thick polyimide-bonded graphite fluoride film. Rider and disk substrate material, 440C HT stainless steel; rider radius, 0.476 centimeter (hemispherically tipped); load, 1 kilogram; sliding speed, 2.6 meters per second (1000 rpm); temperature, 25° C; atmosphere, moist air (10 000 ppm H_2O).

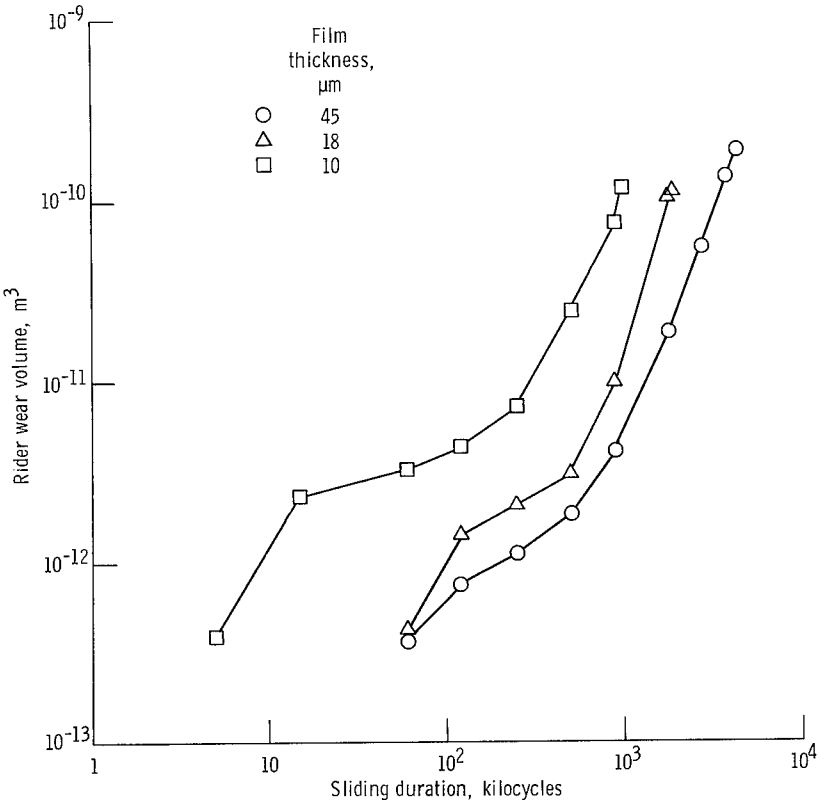

Figure 12. - Rider wear as function of sliding duration for riders sliding on polyimide-bonded graphite fluoride films of three thicknesses. Rider and disk substrate material, 440C HT stainless steel; rider radius, 0.476 centimeter (hemispherically tipped); load, 1 kilogram; sliding speed, 2.6 meters per second (1000 rpm); temperature, 25^0 C; atmosphere, moist air (10 000 ppm H_2O).

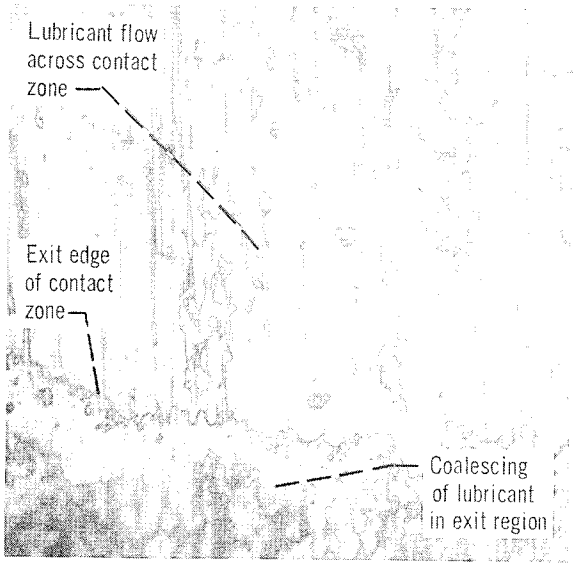

(a) Exit region after 60 kilocycles of sliding.

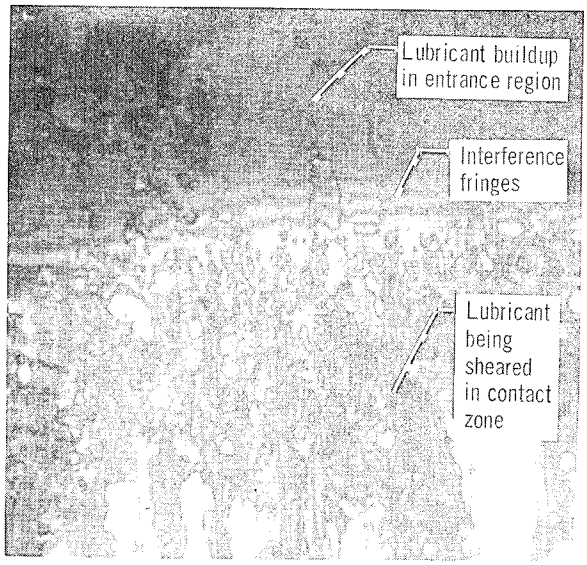

(b) Entrance region after 500 kilocycles of sliding.

(c) Exit region after 900 kilocycles of sliding.

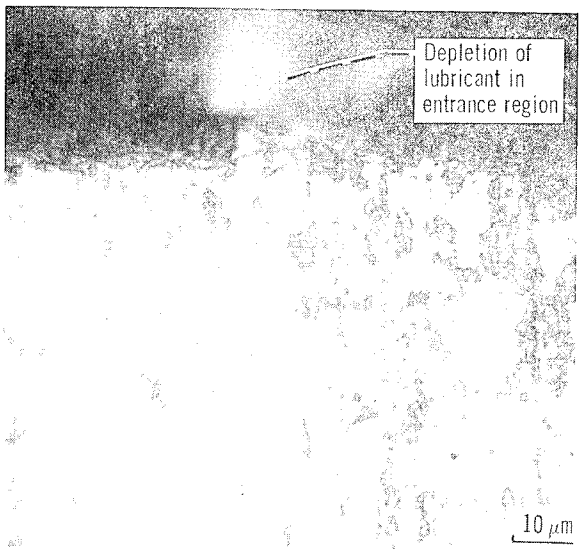

(d) Entrance region after 1800 kilocycles of sliding.

Figure 13. - High-magnification photomicrographs of rider transfer films from figure 11 after 60, 500, 900, and 1800 kilocycles of sliding on polyimide-bonded graphite fluoride films. Rider and disk substrate material, 440C HT stainless steel; rider radius, 0.476 centimeter (hemispherically tipped); load, 1 kilogram; sliding speed, 2.6 meters per second (1000 rpm); temperature, 25° C; atmosphere, moist air (10 000 ppm H_2O).

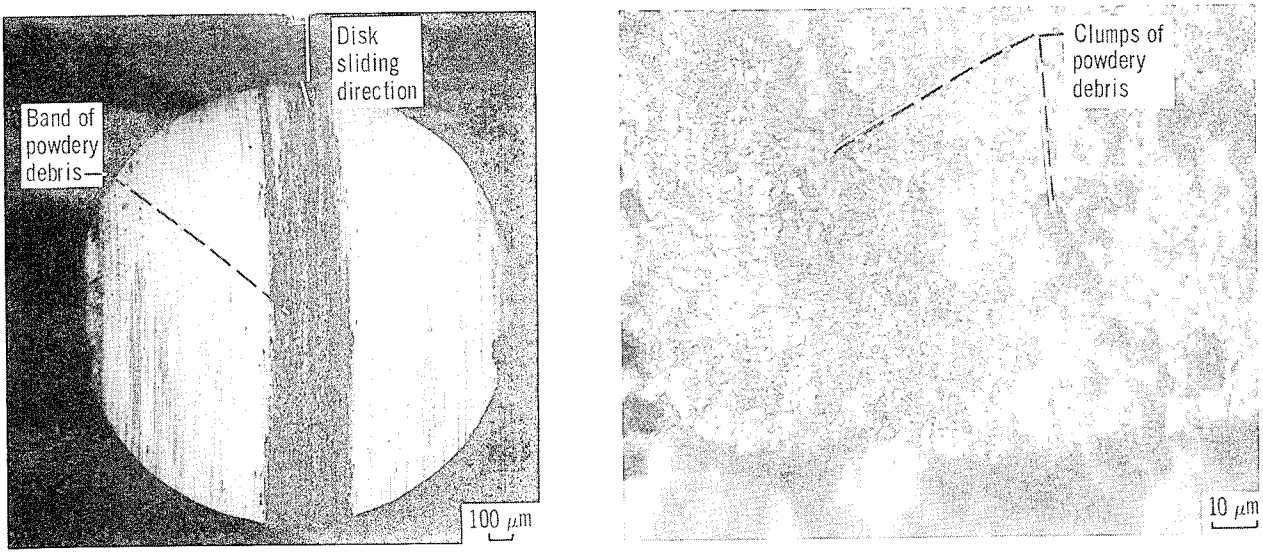

(a) Rider contact area after 4400 kilocycles of sliding.

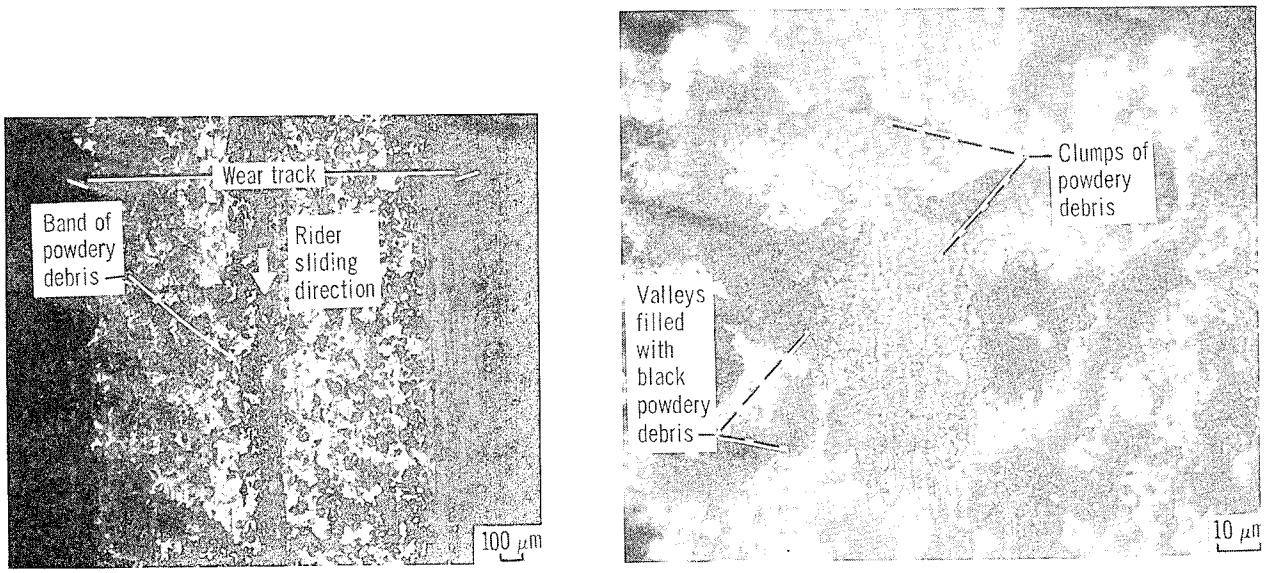

(b) Film wear track after 4400 kilocycles of sliding.

Figure 14. - Photomicrographs of rider contact area and film wear track area after failure (high friction) had occurred. Film thickness, 45 micrometers; rider and disk substrate material, 440C HT stainless steel; rider radius, 0.476 centimeter (hemispherically tipped); load, 1 kilogram; sliding speed, 2.6 meters per second (1000 rpm); temperature, 25° C; atmosphere, moist air (10 000 ppm H_2O).

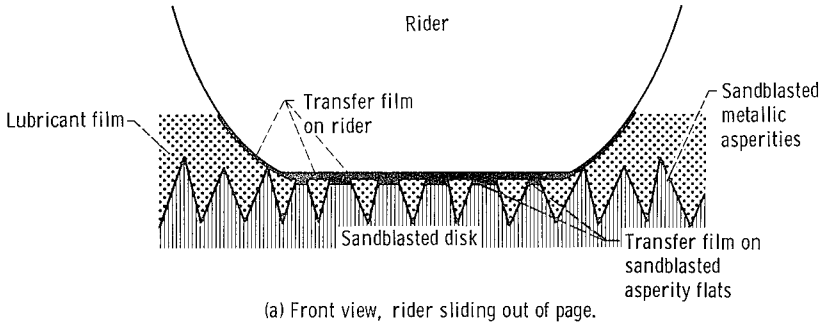

(a) Front view, rider sliding out of page.

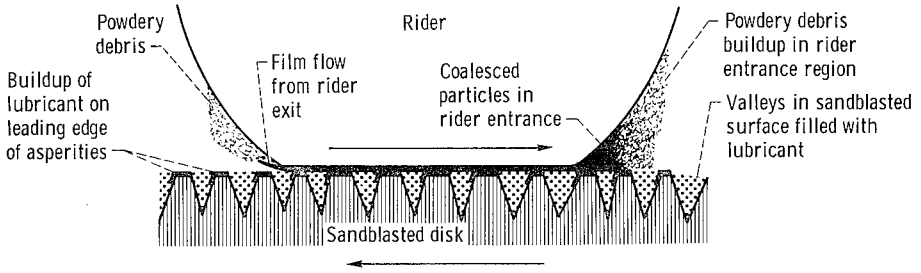

(b) Side view, rider sliding left to right.

Figure 15. - Idealized schematic drawing of sliding surfaces, illustrating lubricating mechanism in the second lubrication regime.

1. Report No. NASA TP-1524	2. Government Accession No.	3. Recipient's Catalog No.
4. Title and Subtitle LUBRICATING AND WEAR MECHANISMS FOR A HEMISPHERE SLIDING ON POLYIMIDE-BONDED GRAPHITE FLUORIDE FILM		5. Report Date August 1979 6. Performing Organization Code
7. Author(s) Robert L. Fusaro		8. Performing Organization Report No. E-9965 10. Work Unit No. 505-04
9. Performing Organization Name and Address National Aeronautics and Space Administration Lewis Research Center Cleveland, Ohio 44135		11. Contract or Grant No. 13. Type of Report and Period Covered Technical Paper
12. Sponsoring Agency Name and Address National Aeronautics and Space Administration Washington, D.C. 20546		14. Sponsoring Agency Code
15. Supplementary Notes		

16. Abstract

Friction, wear life, rider wear, and film wear for a 440C high-temperature-stainless-steel, hemispherically tipped rider sliding against polyimide-bonded graphite fluoride films were evaluated in a moist-air atmosphere at 25° C. Optical microscope and surface profilometry observations were made at various sliding intervals to determine how film thickness affected the lubricating and failure mechanisms of the films. Two lubrication regimes operated for the same load. In the first, the film supported the load and the lubricating mechanism consisted of the shear (plastic flow) of a thin layer of the lubricant between the metallic rider and the film surface. In the second, the film did not support the load (it was worn away) and the lubricating mechanism consisted of the shear of very thin lubricant films between flat areas generated on the rider and on sandblasted metallic asperities in the film wear track. Lubricant was supplied from the valleys between the asperities or from the sides of the wear track. With thicker films, wear life increased since a greater lubricant supply was available from the sides of the wear track.

17. Key Words (Suggested by Author(s))	18. Distribution Statement
Lubricating mechanisms; Solid lubricants; Polyimide; Graphite fluoride; Friction coefficient; Wear mechanisms; Transfer films	Unclassified - unlimited STAR Category 27

19. Security Classif. (of this report)	20. Security Classif. (of this page)	21. No. of Pages	22. Price*
Unclassified	Unclassified	29	A03

* For sale by the National Technical Information Service, Springfield, Virginia 22161

NASA-Langley, 1979